(Article begins on next page)

Preclinical bioassay of a novel antibacterial mesh for the repair of abdominal hernia defects

Barbara P erez-K ohler, BSc, PhD€[a,c,d,*], Selma Benito-Martínez, BSc, PhD[b,c,d], Francisca García-Moreno, MD, PhD[b,c,d], Marta Rodríguez, BSc, PhD[b,c,d], Gemma Pascual, BSc, PhD[a,c,d], Juan M. Bellon, MD, PhD[b,c,d]

[a] Department of Medicine and Medical Specialities, Faculty of Medicine and Health Sciences. University of Alcala. Madrid, Spain [b] Department of Surgery, Medical and Social Sciences. Faculty of Medicine and Health Sciences. University of Alcala, Madrid, Spain [c] Biomedical Research Networking Center on Bioengineering, Biomaterials and Nanomedicine (CIBER-BBN), Madrid, Spain [d] Ramon y Cajal Health Research Institute (IRYCIS), Madrid, Spain

Abstract

Background: In hernia surgery, soaking of meshes in antibiotics before implantation is a prophylactic strategy for minimizing the risk of infection while providing minimal, local, drug doses. This study describes the development and application of an antibacterial mesh coating comprising a carboxymethylcellulose gel loaded with rifampicin in a preclinical model of *Staphylococcus aureus* and *S. epidermidis* infection in rabbits.
Methods: Antibacterial activity and cytocompatibility (with fibroblasts) of unloaded carboxymethylcellulose gel and 0.13 mg/mL rifampicin-carboxymethylcellulose gel were assessed in vitro. Then, partial abdominal wall defects (5 x 2 cm) were created in New Zealand white rabbits (n = 34), the wound inoculated with 0.25 mL of 10^6 CFU *Staphylococcus aureus/ S. epidermidis* (n = 17 each), and the defect then repaired with a lightweight, monofilament, large pore polypropylene mesh either uncoated (n = 3) or coated with carboxymethylcellulose gel (n = 7) or rifampicin-carboxymethylcellulose gel (n = 7). By postoperative day 14, coating performance was evaluated by determining bacterial adhesion (via sonication), host tissue incorporation (via histology), macrophage response via immunostaining), and bloodstream drug diffusion (via high-performance liquid chromatography).
Results: In vitro, rifampicin-carboxymethylcellulose gel demonstrated great activity against *Staphylococcus aureus/S. epidermidis*, while being innocuous for fibroblasts. In vivo, rifampicincarboxymethylcellulose gel-coated implants displayed full bacterial clearance and optimal tissue integration, irrespective of the strain of Staphylococcus. In contrast, uncoated and carboxymethylcellulose gel-coated implants exhibited macro/microscopic signs of infection and impaired tissue integration. Macrophage responses were less in rifampicin-carboxymethylcellulose gel implants than in uncoated mesh (*Staphylococcus aureus/S. epidermidis*; $P < .01$) and carboxymethylcellulose gel (*S. epidermidis*; $P < .05$) implants. Bloodstream levels of rifampicin were undetectable.
Conclusion: Soaking meshes in rifampicin-carboxymethylcellulose gel inhibited effectively the bacterial adhesion to the mesh without compromising the tissue

repair. This antibiotic gel constitutes an easy-touse and effective prophylactic strategy that potentially reduce the prevalence of postoperative mesh infection

Introduction

Over the last few decades, operative procedures aimed at repairing abdominal wall hernias have evolved considerably from the traditional autoplastic tissue reconstruction techniques toward the implantation of prosthetic devices.[1] The results given by Lichtenstein's group demonstrated the low incidence of hernia recurrence using mesh materials,[2] findings that gradually led to the standardization of these devices in the surgical repair of hernia pathology. Notwithstanding, mesh implantation can give rise to a series of postoperative complications, with infection being one of the most devastating.

Mesh infections after hernioplasty cause relevant social, clinical, and economic impacts.[3] According to a recent review, the rate of mesh infection is generally below 1% after inguinal hernia repair, increasing to 3% in laparoscopic incisional repair and to 13% in open incisional repair.[4] These percentages are of great concern given the high frequency of surgical procedures carried out.[5] In hernia repair surgery, most mesh-related infections are triggered by Staphylococcus aureus and S. epidermidis, while other pathogens, such as Escherichia coli, can give rise to infections in complex surgeries involving an enterocutaneous fistula and/or stoma.[6]

The prevalence of mesh infection is mainly related to (i) the type of mesh,[7,8] especially with expanded polytetrafluoroethylene macroporous materials[9] and multifilament polyester meshes,[10] and (ii) patient risk factors.[11] The risk of infection is augmented in those cases where severe complications are present, such as hernia incarceration or strangulation, either with or without bowel resection.[12,13] In those cases, mesh implantation has a great risk of infection.

Before surgery, antibiotic prophylaxis is usually administered to prevent initial or recurrent infections, providing adequate tissue and blood levels of the target antibiotic to avoid bacterial colonization of the implant site.[14e16] Nevertheless, the administration of antibiotics in clean operations is controversial and sometimes not recommended due to the risk of developing allergic reactions to drugs, side effect like diarrhea, or helping to develop bacterial resistance,[17] and consequently, the application of this prophylaxis must be evaluated carefully by clinicians in each specific case.

An alternative for preventing infection consists of avoiding early-onset bacterial colonization of the mesh during surgery, thus inhibiting the adhesion and subsequent formation of the biofilm that keeps bacteria attached to the material surface and protected from the action of drugs and host immune cells.[18] To this

end, different strategies have been developed such as dipping the mesh in antibiotic solutions[19] with controversial opinions on its effectiveness.[20,21] Another option is to coat meshes with antibiotics, such as gentamicin,[22] vancomycin,[23] or rifampicin (RIF). This latter antibiotic has even been incorporated in a collagen-based biomaterial for clinical use,[24,25] with positive outcomes against staphylococcal species.

The manufacturing of these drug-releasing devices is complex, costly, and requires long periods of time, thus limiting their potential application as prophylactic materials in clinical work. Therefore, to provide a simple, cost-effective, and clinically translatable method for endowing meshes with antibacterial activity, we developed a gel-like compound loaded with RIF to be used for the prophylactic soaking of a lightweight, large pore polypropylene mesh. The performance of this coating in preventing staphylococcal infections (S. aureus, S. epidermidis) and its biocompatibility were evaluated first under in vitro conditions and subsequently in vivo using a preclinical, rabbit model of bacterial mesh infection during a mesh-based hernia repair. This novel and easy-to-apply design may have a potential clinical application for patients with a high risk of infection after a mesh-based hernia repair.

Material and methods

In vitro study

Elaboration of the unloaded and antibiotic-loaded gels

To develop the drug-free gel, we used a 1% solution of carboxymethylcellulose sodium (CMC) (Sigma-Aldrich, St. Louis, MO) in ultrapure water. This solution was stirred gently at room temperature until a viscous compound was formed. For the preparation of the antibacterial gel, a stock solution of RIF (15 mg/mL; Sigma-Aldrich) in dimethyl sulfoxide (DMSO) (Sigma-Aldrich) was developed. Then, the stock solution and the CMC were mixed to prepare a 0.13 mg/mL RIF-CMC gel. Both CMC and RIF-CMC gels were prepared under sterile conditions and stored at 4C protected from light until use.

Bacterial strains and preparation of inocula

Two staphylococcal strains from the Spanish Type Culture Collection (Valencia, Spain) were used: S. aureus ATCC25923 (Sa) and S. epidermidis ATCC35984 (Se); neither of these strains were methicillin-resistant. All the inocula prepared contained average loads of 1.25 to 1.50 x 10^6 CFU/mL. Briefly, bacteria were inoculated into 25 mL of lysogeny broth (LB) and incubated overnight at 37C. Then, spectrophotometry (OD600) was used to record the absorbance of cultured bacteria, which were diluted subsequently in sterile 0.9% NaCl until reaching an absorbance equivalent to the target bacterial load. For every inoculum prepared,

the concentration of viable bacteria was determined by the spot plaque method. To avoid cross-contamination, the study was carried out independently for Sa and Se.

Agar well diffusion test

To determine the bactericidal effect of RIF-CMC, an agar well diffusion test was carried out following a previously described protocol.[26] For each strain, 30 LB agar plates were lawn-inoculated with the corresponding Sa/Se inoculum, and circular wells (8 mm diameter x 4 mm depth) were punched in the center of the agar. Then,100 mL of 0.9% NaCl (control), CMC, or RIF-CMC (n ¼ 10 each) was added to the wells, and plates were incubated for 3 days at 37C. At regular 24hour intervals, the plates were scanned for further measurement of the inhibition halo diameters using ImageJ software (National Institutes of Health, Rockville, MD; https://imagej.nih.gov/ij/).

Cell viability

Small biopsies of skin tissue were collected from healthy, male, New Zealand White rabbits (n ¼ 3); male rabbits were chosen to prevent any effects of female sex hormones. Biopsies were transported immediately to the laboratory, and dermal fibroblasts (Fb) were isolated by the explant method, as described previously.[27] Cells were cultured in 6-well plates at a concentration of 2.5 x 10^5 cells/well using Dulbecco's modified Eagle culture medium (DMEM) (Life Technologies, Carlsbad, CA) and a controlled humid atmosphere (37C, 5% CO_2). After overnight culture, media were replaced by fresh DMEM containing a 10% concentration of either CMC or RIF-CMC (n ¼ 9 each). Cells with no treatment and cells exposed to 10% DMSO served as negative and positive controls for toxicity, respectively. Plates were cultured again under a controlled humid atmosphere for 24 hours. Then, the media were replaced with fresh DMEM containing 10% alamarBlue reagent (Bio-Rad Laboratories, Hercules, CA). Plates were incubated for 5 hours, and the absorbance (OD570, OD600) was read using an iMark microplate absorbance reader (Bio-Rad Laboratories). The percentage of cell viability was calculated using specific online software following the manufacturer's instructions (https://www.bio-radantibodies.com/colorimetric-calculator-fluorometric-alamarblue. html). Throughout the study, Fb were monitored with a Zeiss Axiovert 40C phase-contrast microscope (Carl Zeiss, Oberkochen, Germany).

Bacterial adhesion to the mesh surface

This assay was conducted to assess the potential of RIF-CMC to avoid bacterial adhesion to the surface of a mesh material. The lightweight, monofilament, large pore, polypropylene material (Optilene Mesh Elastic; B. Braun, Melsungen, Germany) was used. The basic characteristics of this material are described

below (in vivo section). Under sterile conditions, the mesh was cut into 1 cm^2 fragments which were coated with 200 mL of either CMC or RIF-CMC (n ¼ 4 each, per strain) and transferred into 6-well plates. The same number of uncoated fragments served as a control. Wells were filled with 3 mL of LB broth, inoculated with 1 mL of Sa/Se, and incubated at 37C for 24 hours. Then, the meshes were washed carefully in sterile saline to remove the non-adhered bacteria, fixed in iced 70% ethanol, and stained with 0.25% crystal violet (SigmaAldrich) for 10 minutes at room temperature. Crystal violet is a cationic dye used commonly in the gram-staining method that stains peptidoglycans found in the bacterial cell wall. Grampositive bacteria exhibit a thick layer of peptidoglycans which are stained strongly and acquire a characteristic violet/purple tone. Stained samples were visualized macroscopically to evaluate the bacterial adhesion to the surface of the different meshes.

In vivo preclinical study

Experimental animals and ethics

Thirty-four male, New Zealand White rabbits (3,000 g in weight) were used. Again, male rabbits were used to avoid any potential effects of female sex hormones. The study was carried out in strict accordance with the national and European legislation on the welfare of experimental animals (Spanish Law 6/2013; Spanish Royal Decree 53/2013; European Directive 2010/63/UE; European Convention of the Council of Europe ETS123). All procedures were performed at the University's Animal Research Center which is registered with the Directorate General for Agriculture of the Ministry of Economy and Technology Innovation of the Community of Madrid (ES280050001165), indicating that all facilities legally cover the needs and requirements of the research. The study protocol (registered code: PROEX 160/16) was approved by the University's Committee on the Ethics of Animal Experiments.

Prosthetic material

As in the in vitro part of the study, the biomaterial Optilene Mesh Elastic was used. This is a lightweight (48 g/m^2), large pore, monofilament, polypropylene mesh with a pore size of 7.64 ± 0.32 mm^2. To obtain the meshes for the in vivo study, this material was cut into 5 x 2 cm fragments under sterile conditions.

Experimental design

A total of 34 animals were distributed randomly among the different study groups. Prior to the operation, some of the mesh materials were coated with either CMC or RIF-CMC via immersion of the mesh in the corresponding gel for 10 minutes. All implants were inoculated with Sa or Se. The study groups were then

designed according to mesh coating and inoculating bacteria. The groups were as follows:

Control þ Sa: (n =3) Implants without any treatment and challenged with Sa.

Control þ Se: (n =3) Implants without any treatment and challenged with Se.

CMC þ Sa (n =7) Implants coated with CMC and challenged with Sa.

CMC þ Se (n =7) Implants coated with CMC and challenged with Se.

RIF-CMC þ Sa (n =7) Implants coated with RIF-CMC and challenged with Sa.

RIF-CMC þ Se (n =7) Implants coated with RIF-CMC and challenged with Se.

In the control groups, the number of animals was decreased to comply with the 3Rs criteria for the ethical use of experimental animals (Replacement, Reduction, Refinement).

Operative technique

To minimize pain, 0.05 mg/kg buprenorphine (Buprecare; Divasa Farmavic, Spain) was administered 1 hour before the operation and daily during the first 3 postoperative days. Anesthesia was induced with an intramuscular injection of 70 mg/kg ketamine hydrochloride (Ketolar; Parke-Davis, Spain), 1.5 mg/kg diazepam (Valium; Roche, Spain), and 1.5 mg/kg chlorpromazine (Largactil; Rhone-Poulenc, Spain). Using a sterile technique, a partial hernia^ defect (5 2 cm) was created in the anterior abdominal wall (right lateral side) of the animal, according to a model established by our group[28]; the defect involved the external and internal oblique muscle while sparing the transverse muscle, transversalis fascia, and parietal peritoneum. The defect was inoculated with 0.25 mL of a bacterial suspension containing 10^6 CFU Sa/Se and repaired with either a bare mesh (control group) or a gel-soaked mesh (CMC, RIFCMC groups). The mesh was fixed to the defect edges by a running a 4/0 polypropylene suture interrupted only at the corners of the implant. Skin tissue was closed by simple interrupted stitches with a 3/0 silk suture. All operative procedures were carried out by the same surgeon.

Postsurgical monitoring and sample collection

Animals were submitted daily to visual inspection to monitor any signs of postoperative complications and/or surgical infection. After 14 days postoperatively, the animals were killed via sedation with up to 20 mg/kg of xylazine (Rompun; Bayer, Leverkusen, Germany) plus placement into a CO_2 chamber with increasing concentrations of CO_2 according to the guidelines for experimental animals. Implants were visualized to record macroscopic

evidence of infection, host tissue integration, and vascularization (Table). Then, the implanted mesh plus surrounding host tissue was harvested and cut into sections for further microbiologic and histologic/immunohistochemical assays.

Blood samples were also collected and stored immediately at 4C for further determination of RIF levels in plasma, as described below.

Antibacterial performance of the coatings

A sonication protocol established by our group[26] was carried out to quantify the bacterial adhesion to the implant surface of the different implants using 2 tissue sections per implant. Each fragment comprised the host tissue (along the suture line and muscle underneath the mesh), suture material, implanted mesh, and neoformed connective tissue (with the associated purulent material in those samples involving it). At the time of killing of the animals, tissue was immersed in 20 mL of sterile Neutralizing Pharmacopoeia Diluent (8.5 g NaCl, 2.5 mL Tween-80, 0.35 g soya lecithin, 997.5 mL distilled water) and processed under sterile conditions. Briefly, the mesh was separated from the host tissue and gently scraped with a scalpel blade to tear the tissue capsule and neoformed tissue. Scrapping was also carried out to disrupt the exopolysaccharide matrix of any biofilm that had developed on the mesh surface. Then, the host tissue, suture, scrapped mesh, the rest of neoformed tissue, and the scalpel blade were transferred into the Neutralizing Pharmacopoeia Diluent solution and submitted to sonication (40 KHz) for 10 minutes in a Bransonic 3800-CPXH device (Branson Ultrasonics, Danbury, CT). The sonicated supernatant was vortexed, serially diluted in sterile 0.9% NaCl, plated in LB agar plates, and incubated for 24 hours at 37C. Colonies grown were used to quantify the viable CFU per mesh fragment.

Table
Macroscopic outcomes recorded at euthanasia

Macroscopic outcomes relative to infection					
Skin necrosis	No	Yes*			
Fistula	No	Yes*			
Swelling/edema	No	Soft, small	Soft, large	Hard, small*	Hard, large*
Purulent material	No	Only at the suture line	Implant surface (<25%)	Implant surface (25–50%)*	Implant surface (>50%)*
Macroscopic outcomes relative to tissue repair					
Vascularization	Normal	Slight hypervascularization		Severe hypervascularization*	
Thrombosis	No	Slight		Severe*	
Encapsulation	No	Thin, moderate		Severe*	
Mesh integration	Full	Partial		Delamination*	

*Outcomes entailing a high risk of postoperative infection and/or impaired tissue repair.

Determination of RIF levels in blood plasma

Heparinized blood aspirates were centrifuged at 1,500 g for 15 minutes and 4C using an Eppendorf 5810R centrifuge (Eppendorf AG, Hamburg, Germany). Plasma supernatant was carefully collected, transferred into sterile vials, and stored at e80C. Determination of RIF was carried out via high-performance liquid chromatography (HPLC) at the University's Center for Chemical and Microbiological Analysis. Briefly, plasma samples were deproteinized with acetonitrile (1:1), vortexed, and centrifuged at 9.6 g for 10 minutes. Supernatant aliquots were transferred to vials and analyzed in an Agilent 1200 HPLC (Agilent, Santa Clara, CA) with an X-Terra RP18 column (30 x 150 mm). The mobile phase was a 70:30 mixture of acetonitrile:sodium acetate (50 mmol/L; pH 7.0), and the flow rate was 0.4 mL/min. Measurements were performed at 334 nm. A calibration curve (correlation: 0.99913) was developed using rabbit plasma containing RIF (range 1.87e19.36 mg/mL), and positive controls were measured under the same conditions.

Histologic evaluation

Tissue specimens were used for the evaluation of host tissue integration and implant biocompatibility. Tissue was immersed in F13 fixative solution (60% ethanol, 20% methanol, 7% polyethylene glycol, 13% distilled water), paraffin-embedded, and cut into 5-mm thick sections. Then, the sections were stained with hematoxylineosin and Masson's trichrome (Goldner-Gabe variant) and examined under a Zeiss Axiophot light microscope (Carl Zeiss).

Immunohistochemistry

Immunohistochemical techniques were assessed to determine the macrophage response and the presence of bacteria in the host tissue using paraffin-embedded sections of the different implants. Sections were incubated with monoclonal antibodies against rabbit macrophages RAM-11 (M-633; Dako, Glostrup, Denmark), Sa (ab37644; Abcam, Cambridge, UK), and Se (ab74031; Abcam) in the alkaline phosphatase-labeled avidin-biotin complex method (antibody dilution: 1:50 for RAM-11, 1:500 for Sa/Se). Positive and negative controls exposed to the same conditions as the experimental samples were used to set up the detection threshold of these techniques. Tissue slides from a non-infected, polypropylene implant and glass coverslips inoculated with Sa/Se served as positive controls for RAM-11 and bacteria immunolabeling, respectively. Negative controls consisted of tissue slides from the implants to be analyzed, which were incubated in the absence of the primary antibodies. For each sample, labeled macrophages were quantified by counting 8 light microscopy fields (200) taken randomly from one margin of the defect to the

opposite one, to determine the percentage of positively stained cells out of the total number of cell nuclei. The presence of Sa/Se was visually evaluated.

Statistical análisis

Data collected were compared among the different experimental groups tested using the Mann-Whitney U test. Data are provided as the mean ± standard error of the mean. All statistical tests were performed using the GraphPad Prism 5 computer package (GraphPad Software Inc, La Jolla, CA). The statistical level for significance was set at $P < .05$.

Results

In vitro antibacterial activity

As expected, the control and CMC groups did not exert any antibacterial activity. In contrast, wide inhibition halos developed with the treatment with RIF-CMC (Fig 1, A). By day 1, the amplitude of these halos (Sa: 40 ± 1 mm; Se: 46 ± 1 mm) was wider for Se than for Sa ($P < .001$), and the results remained unaltered during the 3day period of study. No bacterial growth within the inhibition zone was recorded, suggesting satisfactory biocide activity of this antibiotic gel.

Consistent with these data, the results from the crystal violet staining revealed strong bacterial adhesion to the surface of the uncoated and CMC meshes (Fig 1, B), especially after challenge with Sa. In these groups, bacterial biofilms covered most of the mesh surface and exhibited acute staining, suggesting the presence of a staphylococcal biomass with great affinity to polypropylene-based materials. All samples from the RIF-CMC group appeared fully unstained, revealing a lack of Sa/Se adhesion to the surface of these treated materials.

In vitro gel cytocompatibility

The addition of CMC and RIF-CMC to the culture media did not provoke any adverse effects to the Fb, whose shape appeared similar to that observed from the untreated control cells (Fig 2, A), while the exposure to 10% DMSO (positive control for toxicity) provoked surface detachment and apoptosis of almost all the cells. Likewise, the alamarBlue test (Fig 2, B) revealed similar percentages of cell viability among the control (99.9 ± 1.6%), CMC (91.7 ± 2.4%), and RIF-CMC (92.1 ± 1.6%) groups. Only the DMSO-treated Fb (22.1 ± 3.6%) exhibited relevant signs of toxicity with respect to the rest of the experimental groups ($P < .001$).

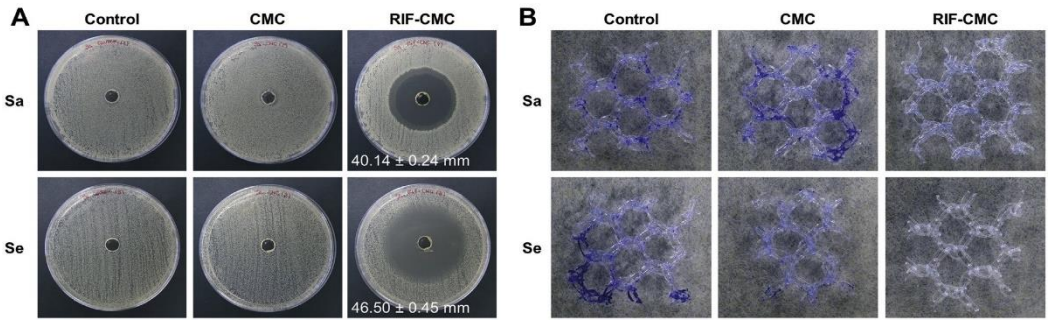

Fig 1. In vitro performance of the gels after 24 hours of bacterial inoculation. Pictures are representative of the different study groups. (A) Only the RIF-CMC treatment resulted in inhibition halos against the Sa and Se strains, as observed with the agar well diffusion test. (B) Crystal violet staining of Sa/Se-inoculated meshes revealed strong adhesion to the uncoated (control) and CMC-coated meshes, while meshes treated with RIF-CMC displayed a surface free of bacteria.

Postoperative follow-up

There was no mortality in any of the study groups. Regardless of the inoculating bacteria, daily monitoring of the animals revealed an absence of postoperative complications such as wound dehiscence or mesh displacement, as well as any other physical manifestations, such as skin erythema, necrosis, or edema. Once the end of the study (14 days) was reached, however, early signs of sinus formation were recorded for 1 Sa-inoculated (CMC group) and 2 Seinoculated (control and CMC groups) animals. During the second postoperative week, animals from the control and CMC groups developed small bulges under the skin that were soft to the touch and slightly increased in size over the ensuing days. These bulges appeared in areas close to the laparotomy incision, were more perceptible in those specimens inoculated with Sa, and suggested the development of abscesses in the area of the implant. Contrary to these observations, animals from the RIF-CMC groups did not exhibit any similar signs of postoperative complications.

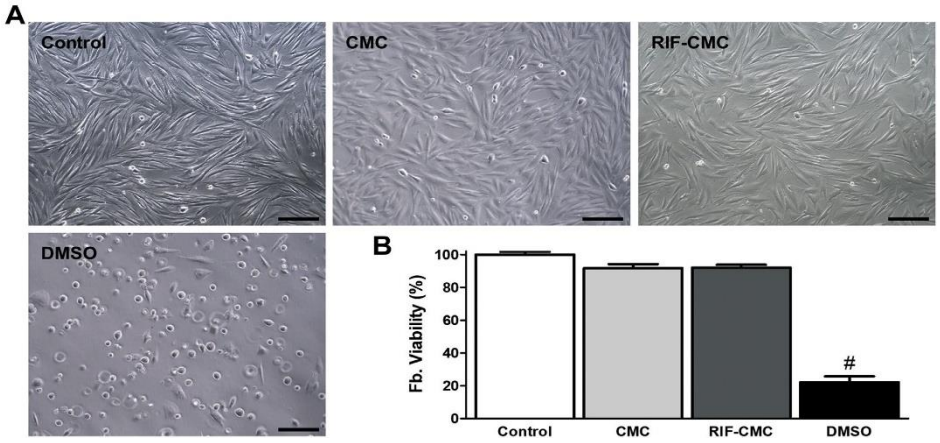

Fig 2. In vitro cytocompatibility of the gels. (A) Phase-contrast light microscopic images of rabbit fibroblasts (Fb) after 24 hours exposure to the different treatments (100). Both CMC and RIF-CMC gels appeared to be innocuous, without provoking any detrimental effects to cultured cells in comparison with a positive control for cell toxicity, such as DMSO. (B) Determination of the cell viability. #: P < .001 versus all groups.

Macroscopic findings and bacterial adhesion to the implant surface

Overall, the response to infection was similar between the 2 control groups as well as between the 2 CMC groups, although Sa triggered a more severe infection than did Se (Fig 3, A). Irrespective of the inoculating bacteria, uncoated control meshes were surrounded by a fibrous capsule with moderate vascularization over the implant. These implants displayed several aggregates of purulent material covering different areas of the mesh surface. Observations from the CMC implants were comparable to those from the control group, although thinner fibrous encapsulation and milder signs of infection were recorded. In contrast, the RIF-CMC implants displayed a mesh surface free of any purulent material, revealing the adequate performance of the antimicrobial coating. In this latter group, a turbid exudate was collected from 2, Sa-inoculated specimens, and further microbiologic tests revealed the absence of bacteria in this fluid.

Quantification of bacterial adhesion to the implant surface via sonication (Fig 3, B) revealed equivalent bacterial yields for the control and CMC implants regardless of the inoculating strain. These loads decreased to 0 in the RIF-CMC implants against both the Sa (P < .001) and Se exposures (P < .01). Consistent with the macroscopic observations, the number of bacteria from the Sainoculated implants were greater than those from Se, both in the control (P < .01) and in the CMC (P < .01) groups.

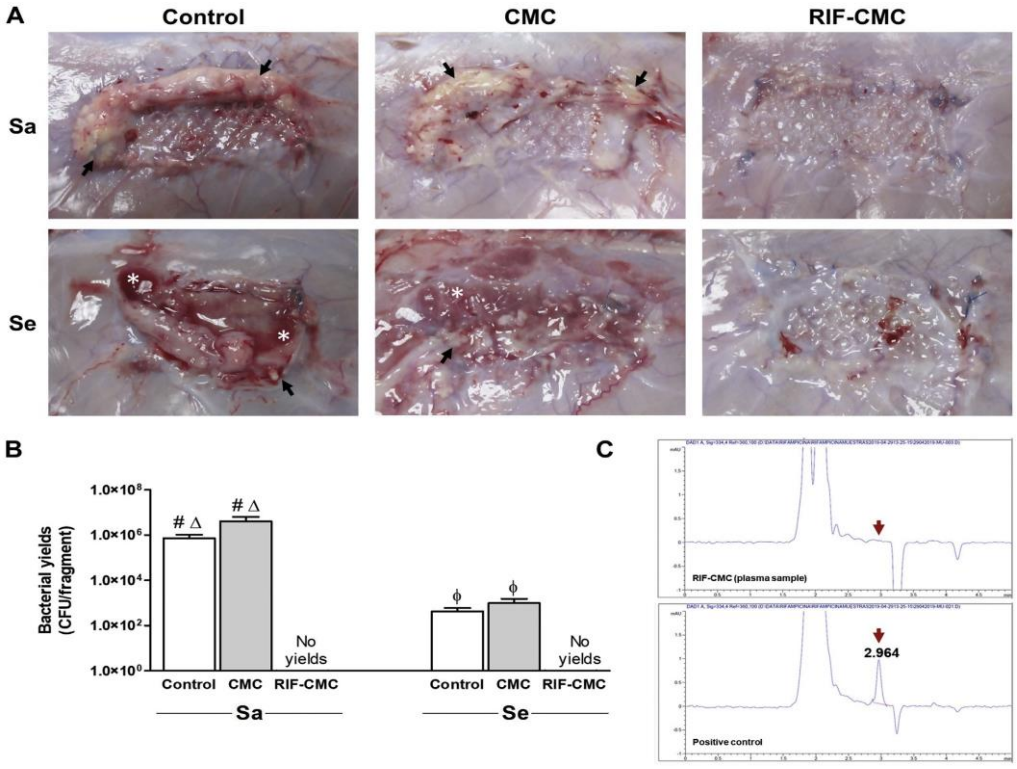

Fig 3. Response of the different implants to infection after 14 days of Sa/Se inoculation. (A) Macroscopic observations at the time of killing of the rabbits, with evidence of purulent material deposits (/) and fluid exudate (*) along the surface of non-treated and CMC implants, but not in RIF-CMC implants. (B) Quantification of bacteria yielded from the different implants via sonication. #: P < .001 versus RIF-CMC; ϕ: P < .01 versus RIF-CMC; D: P < .01 versus Sa/Se inoculated groups. (C) Chromatograms from the HPLC assays revealing undetectable levels of the drug in plasma samples from the RIF-CMC group. By contrast, the presence of RIF was detected in all the positive controls tested

Plasma levels of drug

Plasma collected from the different animals undergoing RIFCMC implants was analyzed via HPLC to determine the presence of antibiotic in the bloodstream. In all samples, the plasma concentration of RIF was less than the lower limit of quantification of the HPLC technique (0.20 mg/mL), indicating no systemic diffusion of the drug into the circulation (Fig 3, C).

Histologic findings

Light microscopic observations from the Sa-inoculated (Fig 4) and Se-inoculated implants (Fig 5) revealed striking differences among the study groups. Uncoated control implants displayed several abscesses embedded in a dense, neoformed

connective tissue, which were particularly large in those specimens challenged with Sa. In all these implants, impaired integration of the mesh was evident, especially in the proximity of the abscesses. Throughout the infected tissue, different amounts of cell debris were visualized, as well as the presence of inflammatory and foreign body giant cells. Immunohistochemical techniques targeting Sa and Se located these bacteria within the abscesses and in the areas of the neoformed tissue adjacent to the mesh filaments. Observations from the CMC groups were similar with the challenge with Sa, although milder signs of infection were recorded in the Se-inoculated implants, where dispersed microabscesses and better tissue integration were recorded. Contrary to all these observations, findings from the RIF-CMC groups showed complete bacterial clearance regardless of the inoculating bacteria. These implants were fully integrated into a loose connective tissue that infiltrated the mesh pores in a concentric fashion.

The results from the macrophage response showed the presence of RAM-11-positive cells distributed mainly surrounding the mesh filaments in all the groups (Fig 6, A), which were specifically evident in the uncoated control implants. Labeled cells were also evidenced within and surrounding the abscesses. Regardless of the inoculating bacteria, implants from the control and CMC groups exhibited a greater number of macrophages distributed along the neoformed connective tissue compared to the RIF-CMC implants. In alignment with this, quantification of these cells (Fig 6, B) revealed lesser macrophage responses in the RIF-CMC implants than in the control groups inoculated with either Sa ($P < .01$) or Se ($P < .01$). Furthermore, RIF-CMC implants displayed a lesser percentage of RAM-11-labeled cells than CMC implants, being statistically significant only with the challenge with Se ($P < .05$).

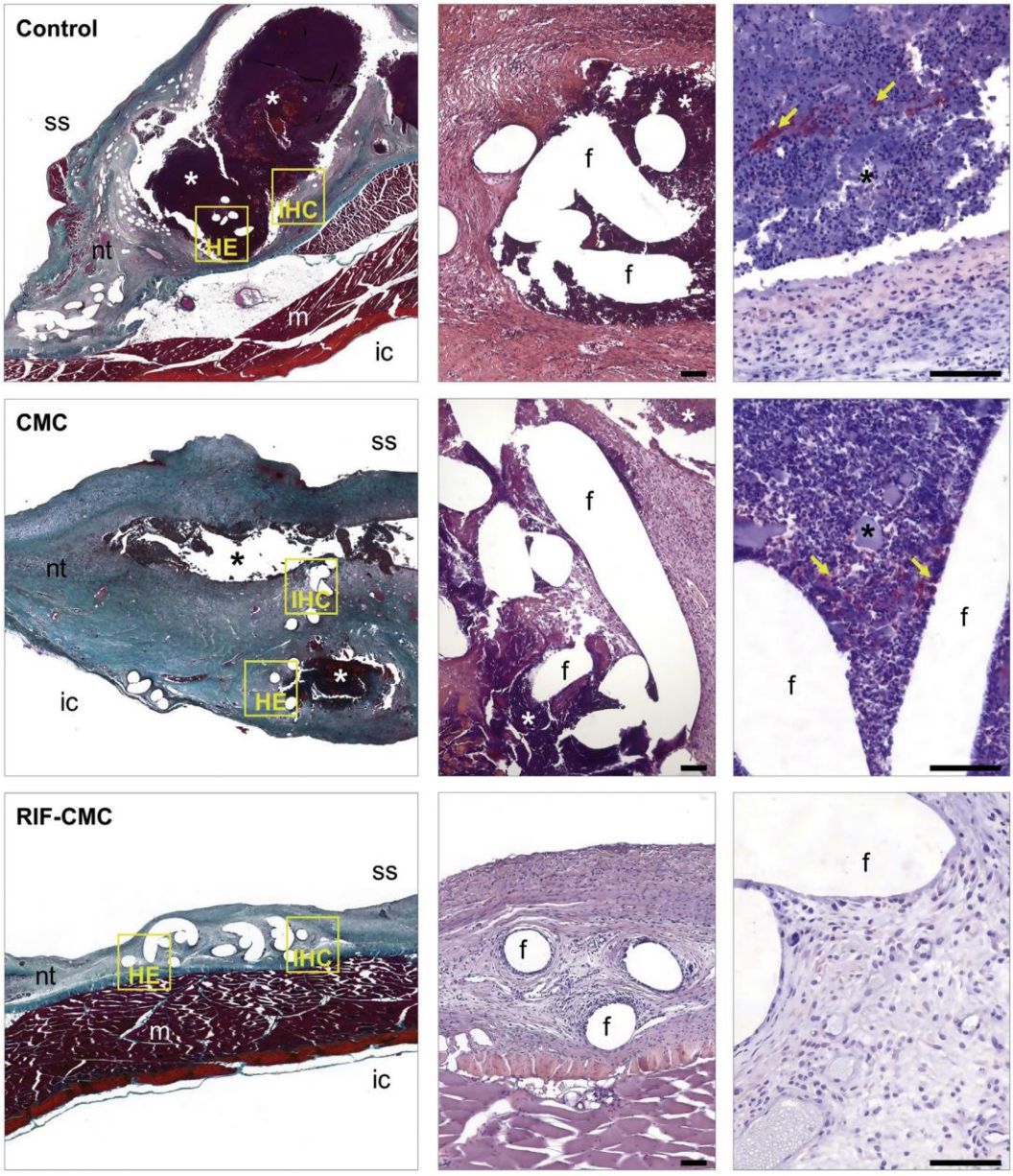

Fig 4. Histological findings of the Sa-inoculated control, CMC, and RIF-CMC implants. For each group, a panoramic composition of the implant is illustrated (Masson's trichrome, x50). Boxes depicted in this composition locate the areas detailed in the subsequent hematoxylin-eosin (HE, 100) and Sa-immunostaining (IHC, 320) pictures. Scale bars: 100 mm.

Symbols: (ic) intraperitoneal cavity; (f) mesh filaments; (m) muscle; (nt) neoformed tissue; (ss) subcutaneous side; (*) abscess; (/) bacteria

Discussion

As with other interfaces, such as orthopedic[29] or vascular[30] surgery, mesh-related infections after hernia repair are a growing complication of great concern, mainly due to the high frequency of operative interventions performed worldwide. Far from decreasing, primary incisional hernias have maintained their rates of population-based incidence; neither laparoscopic nor robotic surgery is able to eliminate this problem, because new hernias are often provoked as a result of trocar penetration into the abdominal cavity.31,32

Due to the scarcity of prospective clinical studies, current literature reports related to mesh-associated infections are difficult to evaluate. First, the inflammatory process triggered by the developing infection is not always considered. Second, surgical site infection eventually overlaps with the mesh infection. Third, data bias is generated when patients exhibiting postoperative infections seek medical consultation with surgeons/hospitals other than those who operated on them the first time. Together, these facts explain the wide range of data available and thus the difficulty of establishing truly accurate rates of mesh infection.

As mentioned before, postoperative mesh infection is mainly related to the implanted biomaterial, its interaction with bacteria, and the patient's host immune system.[18,33] To combat this problem, pretreatment of meshes with antimicrobials is a strategy currently being developed. If bacterial adhesion is precluded, the process of mesh integration will take place smoothly, and instead of bacteria, host cells will colonize the implant surface, as described by Gristina et al in the so-called “race for the surface.”[34]

Antimicrobial coatings for medical devices loaded with either antibiotics or antiseptics must meet the following requirements: (i) provide a local and sustained release of drugs into the operative area, (ii) avoid any detrimental effects, such as toxicity or allergies, in host cells/tissues, and (iii) lack the impacts of a systemic drug.[23,35] This latter condition is key to avoiding the worrisome and increasingly present development of bacterial resistance to antibiotics. According to these requisites, we developed a biocompatible, antibiotic-loaded compound for the prophylactic coating of polypropylene meshes, validating its performance under in vitro and in vivo conditions.

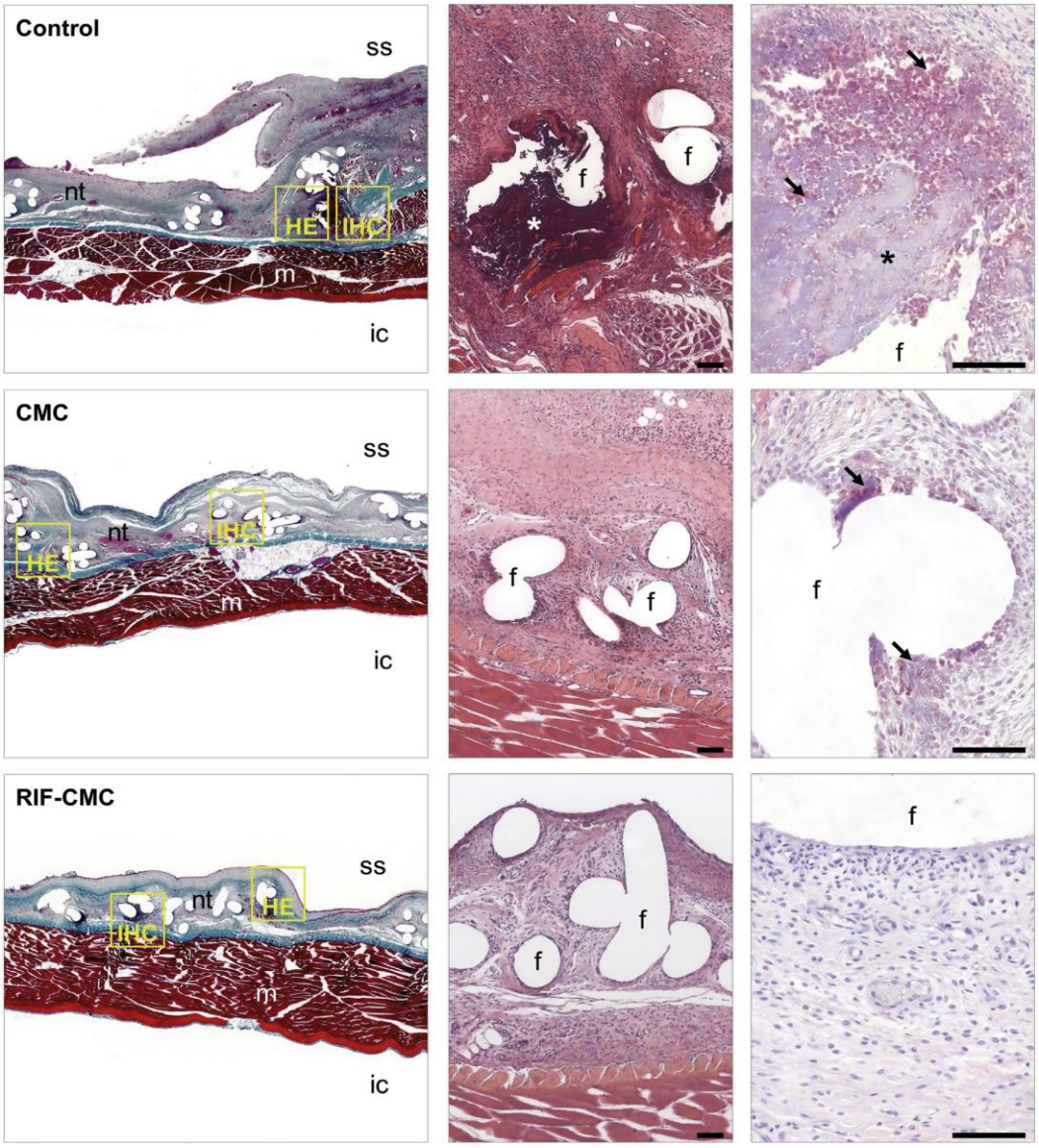

Fig 5. Histologic findings of the Se-inoculated control, CMC, and RIF-CMC implants. For each group, a panoramic composition of the implant is illustrated (Masson's trichrome, 50). Boxes depicted in this composition locate the areas detailed in the subsequent hematoxylin-eosin (HE, 100) and Se-immunostaining (IHC, 320) pictures. Scale bars: 100 mm. Symbols: (ic) intraperitoneal cavity; (f) mesh filaments; (m) muscle; (nt) neoformed tissue; (ss) subcutaneous side; (*) abscess; (/) bacteria.

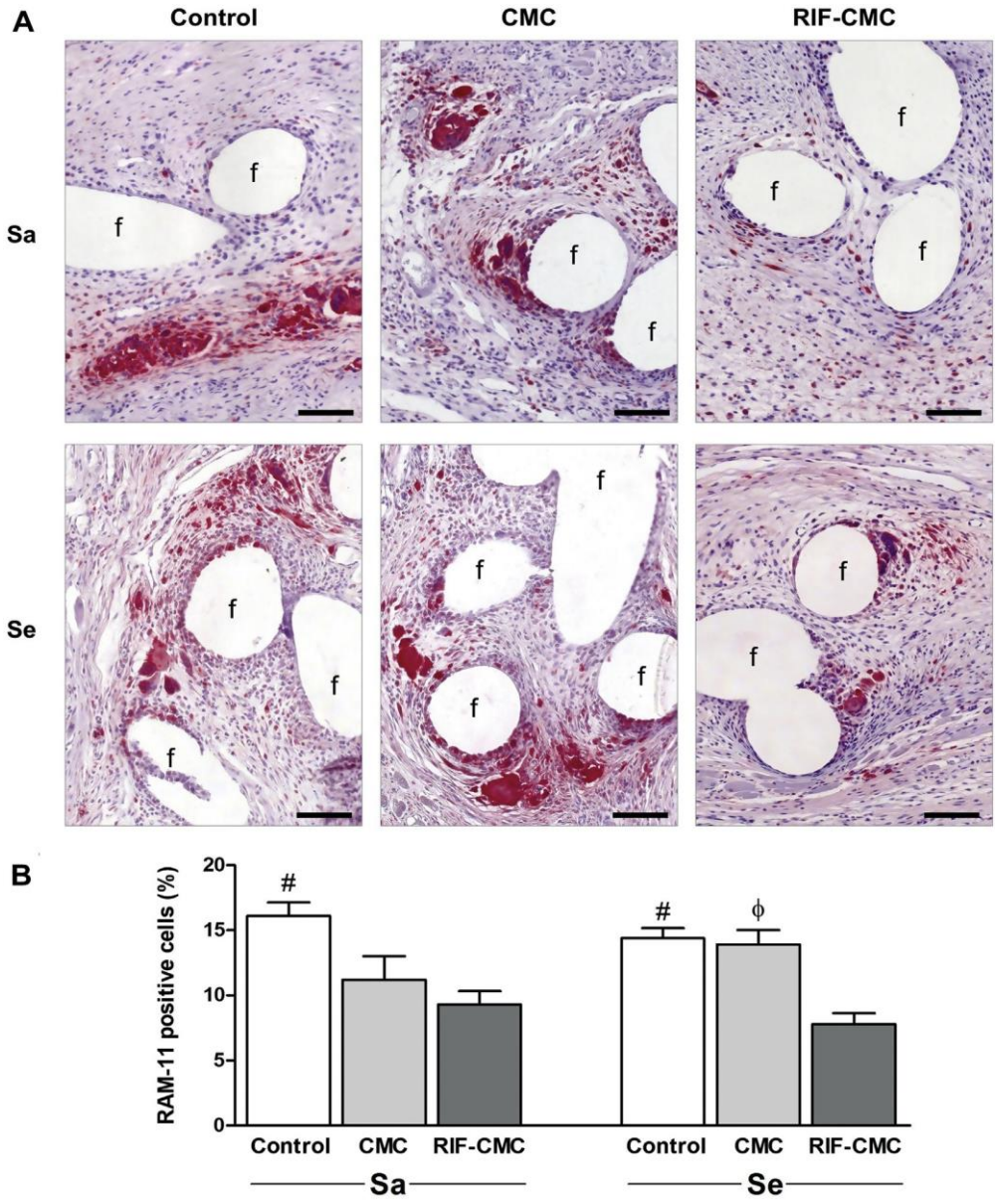

Fig 6. Macrophage reaction. (A) RAM-11 immunostaining (x200) of the control, CMC, and RIF-CMC implants challenged with Sa and Se, showing the presence and distribution of labeled (red-stained cells) macrophages and foreign body giant cells throughout the neoformed tissue. (B) Quantification of the percentage of RAM-11-positive cells quantified in the different study groups. #: $P < .01$ versus RIF-CMC; ϕ: $P < .05$ versus RIF-CMC.

It is well known that the presence of an implanted foreign body decreases by approximately 4-log the minimum bacterial load required to trigger a biomaterial-related infection after hernia repair;[10,36] indeed, according to published data, 10^2 CFU loads are sufficient to develop infections in this scenario.[37] Our experimental model comprised bacterial loads up to 10^6 CFU, which are greater than the loads usually found clinically[38]; our aim was to provoke acute infections that would allow us to evaluate the performance, security, and potential application of the antimicrobial compound developed.

The selected drug, RIF, has been considered recently to be an optimal antibiotic for the prophylactic coating of hernia mesh materials due to its bactericidal activity and liposoluble characteristics.[39] We determined the dose of RIF loaded in the gel (0.13 mg/ mL) by titration of the antibacterial activity and cytocompatibility of several concentrations ranging from 1 mg/mL to 0.01 mg/mL, by means of the inhibition halos and cell viability tests. After the coating process, approximately, 50 mL of gel were impregnated onto 1 cm^2 of the polypropylene mesh. This means that coating the mesh with a 0.13 mg/mL CMC-RIF gel was designed to provide on the material about 6.5 mg of RIF per 1 cm^2.

In a retrospective study comprising 278 patients, the effectiveness of applying RIF onto a mesh before performing a tension-free inguinal hernia repair was evaluated.[40] The drug (250 mg) was applied topically onto polypropylene meshes, and a follow-up of 6 to 36 months was analyzed, comparing treated patients (n ¼ 134) with placebo patients (n ¼ 144). The results showed a significantly lesser infection rate in those patients receiving RIF, and no allergic reactions to this antibiotic were recorded. Consistent with these data, our findings revealed a potent biocidal activity of the RIFloaded gel against the 2 staphylococcal strains tested. With no additional prophylaxis administered, the antibiotic coating applied to the meshes achieved full bacterial clearance. Together with this finding, neither local toxicity nor systemic drug diffusion were recorded, demonstrating the effective performance of this prophylactic strategy.

Biocompatibility is another key feature to be considered when assessing the performance of mesh coatings. Generally, mesh implantation triggers a tissue repair process in which several events occur, such as the activation/migration of granulocytes, macrophages, and foreign body giant cells to the damaged area, fibroblast infiltration into the interstices of the pores of the meshed material, neovascularization, and synthesis of new extracellular matrix.[41] On infection, tissue repair is altered, giving rise to the development of a fibrous capsule that surrounds the implant and hampers mesh integration and even the action of antimicrobial drugs.[42,43] Not only did our antimicrobial coating markedly decrease the fibrous encapsulation but also triggered a significantly lesser macrophage

response than did the other implants, indicating the optimal biocompatibility of this compound. Together with the macrophage response, the evaluation of neutrophils in these implants would have provided relevant information to better understand the inflammatory reaction developed in this short-term mode of infection, given the close relationship and coordination between these 2 cell lineages.[44]

In addition to the strong antibacterial activity and biocompatibility, other advantages of this prophylactic coating, such as its versatility and applicability, deserve mention and are some of the key properties to be considered for the development of the "ideal" mesh material.[45] The processing of this drug-loaded gel is relatively easy, uncomplicated, and cost-effective, and the soaking of meshes in this compound provides an immediate antibacterial barrier. Given its optimal properties as a coating agent, this gel-like solution could potentially be translated into clinical work, for example, in the form of a ready-to-use kit to soak all meshed materials for hernia repair, irrespective of their architecture or chemical composition.

Although promising, we must highlight that the results described in this study were collected from a preclinical study comprising a predetermined number of experimental animals and well-characterized ATCC bacterial strains. An increase in sample sizes as well as the evaluation of this gel coating on challenge with more virulent bacterial strains, (ie, clinical isolates, methicillinresistant-bacteria, etc), would allow us to observe a greater number of outcomes in order to determine more in depth the performance and potential clinical application of the RIF-loaded CMC for prophylactic coating of hernia repair mesh materials.

In conclusion, in a setting of a staphylococcal infection, the prophylactic soaking of large pore, monofilament polypropylene mesh in a CMC loaded with RIF averts bacterial adhesion and colonization of the implant site in this rabbit model, without hampering the tissue repair and mesh integration processes. Its ease of use, local antibacterial efficacy, and biocompatibility indicate a potential clinical application of this gel coating for the prevention of postoperative infections after mesh-based hernia repairs.

Funding/Support

This study was supported by a grant (SAF2017e89481-P) from the Spanish Ministry of Science, Innovation, and Universities.

Conflict of interest/Disclosure

The authors have no personal or financial conflicts of interest to declare.

References

1. Towfigh S. Inguinal hernia: four open approaches. Surg Clin North Am. 2018;98: 623e636.
2. Lichtenstein IL, Shulman AG, Amid PK, Montllor MM. The tension-free hernioplasty. Am J Surg. 1989;157:188e193.
3. Robinson TN, Clarke JH, Schoen J, Walsh MD. Major mesh-related complications following hernia repair: events reported to the Food and Drug Administration. Surg Endosc. 2005;19:1556e1560.
4. Montgomery A, Kallinowski F, Ko€ckerling F. Evidence for replacement of an infected synthetic by a biological mesh in abdominal wall hernia repair. Front Surg. 2016;2:67.
5. Rutkow IM. Demographic and socioeconomic aspects of hernia repair in the United States in 2003. Surg Clin North Am. 2003;83:1045e1051.
6. Yegiyants S, Tam M, Lee DJ, Abbas MA. Outcome of components separation for contaminated complex abdominal wall defects. Hernia. 2012;16:41e45.
7. Engelsman AF, van der Mei HC, Ploeg RJ, Busscher HJ. The phenomenon of infection with abdominal wall reconstruction. Biomaterials. 2007;28: 2314e2327.
8. Engelsman AF, van der Mei HC, Busscher HJ, Ploeg RJ. Morphological aspects of surgical meshes as a risk factor for bacterial colonization. Br J Surg. 2008;95: 1051e1059.
9. Bellon JM, García-Carranza A, García-Honduvilla N, Carrera-San Martín A, Bujan J. Tissue integration and biomechanical behaviour of contaminated experimental polypropylene and expanded polytetrafluoroethylene implants. Br J Surg. 2004;91:489e494.
10. Klinge U, Junge K, Spellerberg B, Piroth C, Klosterhalfen B, Schumpelick V. Do multifilament alloplastic meshes increase the infection rate? Analysis of the polymeric surface, the bacteria adherence, and the in vivo consequences in a rat model. J Biomed Mater Res. 2002;63:765e771.
11. Sanchez VM, Abi-Haidar YE, Itani KM. Mesh infection in ventral incisional hernia repair: incidence, contributing factors, and treatment. Surg Infect (Larchmt). 2011;12:205e210.
12. Xourafas D, Lipsitz SR, Negro P, Ashley SW, Tavakkolizadeh A. Impact of mesh use on morbidity following ventral hernia repair with a simultaneous bowel resection. Arch Surg. 2010;145:739e744.
13. Venara A, Hubner M, Le Naoures P, Hamel JF, Hamy A, Demartines N. Surgery for incarcerated hernia: short-term outcome with or without mesh. Langenbecks Arch Surg. 2014;399:571e577.
14. Sanabria A, Domínguez LC, Valdivieso E, Gomez G. Prophylactic antibiotics for mesh inguinal hernioplasty: a meta-analysis. Ann Surg. 2007;245:392e396.

15. Enzler MJ, Berbari E, Osmon DR. Antimicrobial prophylaxis in adults. Mayo Clin Proc. 2011;86:686e701.
16. Tubre DJ, Schroeder AD, Estes J, Eisenga J, Fitzgibbons Jr RJ. Surgical site infection: the "Achilles Heel" of all types of abdominal wall hernia reconstruction. Hernia. 2018;22:1003e1013.
17. Ko€ckerling F. Antibiotic prophylaxis in laparoendoscopic hernia surgery. Int J Abdom Wall Hernia Surg. 2018;1:9e12.
18. Engelsman AF, van Dam GM, van der Mei HC, Busscher HJ, Ploeg RJ. In vivo evaluation of bacterial infection involving morphologically different surgical meshes. Ann Surg. 2010;251:133e137.
19. Deysine M. Pathophysiology, prevention, and management of prosthetic infections in hernia surgery. Surg Clin North Am. 1998;78:1105e1115.
20. Falagas ME, Kasiakou SK. Mesh-related infections after hernia repair surgery. Clin Microbiol Infect. 2005;11:3e8.
21. Yabanoglu H, Arer I_M, Çalıskan K. The effect of the use of synthetic mesh soaked in antibiotic solution on the rate of graft infection in ventral hernias: a prospective randomized study. Int Surg. 2015;100:1040e1047.
22. Junge K, Rosch R, Klinge U, et al. Gentamicin supplementation of polyvinylidenfluoride mesh materials for infection prophylaxis. Biomaterials. 2005;26:787e793.
23. Fernandez-Gutierrez M, Olivares E, Pascual G, Bellon JM, San Roman J. Lowdensity polypropylene meshes coated with resorbable and biocompatible hydrophilic polymers as controlled release agents of antibiotics. Acta Biomater. 2013;9:6006e6018.
24. Baker EH, Lepere D, Lundgren MP, et al. Early clinical outcomes of a novel antibiotic-coated, non-crosslinked porcine acellular dermal graft after complex abdominal wall reconstruction. J Am Coll Surg. 2016;223:581e586.
25. Majumder A, Scott JR, Novitsky YW. Evaluation of the antimicrobial efficacy of a novel rifampin/minocycline-coated, noncrosslinked porcine acellular dermal matrix compared with uncoated scaffolds for soft tissue repair. Surg Innov. 2016;23:442e455.
26. Perez-Ko€hler B, Fernandez-Gutierrez M, Pascual G, García-Moreno F, San Roman J, Bellon JM. In vitro assessment of an antibacterial quaternary ammonium-based polymer loaded with chlorhexidine for the coating of polypropylene prosthetic meshes. Hernia. 2016;20:869e878.
27. Bellon JM, Rodríguez M, Perez-Ko€hler B, Perez-Lopez P, Pascual G. The New Zealand white rabbit as a model for preclinical studies addressing tissue repair at the level of the abdominal wall. Tissue Eng Part C Methods. 2017;23: 863e880.
28. Perez-Ko€hler B, García-Moreno F, Brune T, Pascual G, Bellon JM. Preclinical bioassay of a polypropylene mesh for hernia repair pretreated with antibacterial solutions of chlorhexidine and allicin: an in vivo study. Plos One. 2015;10:

e0142768.
29. Beam E, Osmon D. Prosthetic joint infectionupdate. Infect Dis Clin North Am. 2018;32:843e859.
30. Gharamti A, Kanafani ZA. Vascular graft infections: an update. Infect Dis Clin North Am. 2018;32:789e809.
31. Swank HA, Mulder IM, la Chapelle CF, Reitsma JB, Lange IF, Bemelman WA. Systematic review of trocar site hernia. Br J Surg. 2012;99:315e323.
32. Harr JN, Juo YY, Luka S, Agarwal S, Brody F, Obias V. Incisional and port-site hernias following robotic colorectal surgery. Surg Endosc. 2016;30: 3505e3510.
33. Perez-Ko€hler B, Bayon Y, Bellon JM. Mesh infection and hernia repair: a review. Surg Infect (Larchmt). 2016;17:124e137.
34. Gristina AG, Naylor P, Myrvik Q. Infections from biomaterials and implants: a race for the surface. Med Prog Technol. 1988-1989;14:205-224.
35. Guillaume O, Lavigne JP, Lefranc O, Nottelet B, Coudane J, Garric X. New antibiotic-eluting mesh used for soft tissue reinforcement. Acta Biomater. 2011;7:3390e3397.
36. Halaweish I, Harth K, Broome AM, Voskerician G, Jacobs MR, Rosen MJ. Novel in vitro model for assessing susceptibility of synthetic hernia repair meshes to Staphylococcus aureus infection using green fluorescent protein-labeled bacteria and modern imaging techniques. Surg Infect (Larchmt). 2010;11: 449e454.
37. Sanders DL, Kingsnorth AN, Lambie J, Bond P, Moate R, Steer JA. An experimental study exploring the relationship between the size of bacterial inoculum and bacterial adherence to prosthetic mesh. Surg Endosc. 2013;27: 978e985.
38. Alexiou K, Drikos I, Terzopoulou M, Sikalias N, Ioannidis A, Economou N. A prospective randomised trial of isolated pathogens of surgical site infections (SSI). Ann Med Surg (Lond). 2017;21:25e29.
39. Reinbold J, Hierlemann T, Urich L, et al. Biodegradable rifampicin-releasing coating of surgical meshes for the prevention of bacterial infections. Drug Des Devel Ther. 2017;11:2753e2762.
40. Kahramanca S¸ , Kaya O, Azılı C, Celep B, Go€kce E, Küçükpınar T. Does topical rifampicin reduce the risk of surgical field infection in hernia repair? Ulus Cerrahi Derg. 2013;29:54e58.
41. Offner FA, Klosterhalfen B. Pathology of infected mesh. In: Deysine M, ed. Hernia Infections: Pathophysiology, diagnosis, treatment and prevention. 1st ed. Boca Raton (FL): CRC Press; 2003:56e73.
42. Buret A, Ward KH, Olson ME, Costerton JW. An in vivo model to study the pathobiology of infectious biofilms on biomaterial surfaces. J Biomed Mater Res. 1991;25:865e874.

43. Bueno-Lledo J, Torregrosa-Gallud A, Sala-Hernandez A, et al. Predictors of mesh infection and explantation after abdominal wall hernia repair. Am J Surg. 2017;213:50e57.
44. Prame Kumar K, Nicholls AJ, Wong CHY. Partners in crime: neutrophils and monocytes/macrophages in inflammation and disease. Cell Tissue Res. 2018;371:551e565.
45. Binnebo€sel M, von Trotha KT, Jansen PL, Conze J, Neumann UP, Junge K. Biocompatibility of prosthetic meshes in abdominal surgery. Semin Immunopathol. 2011;33:235e243.